ChemComm
FEATURE ARTICLE

Panoscopic materials: synthesis over 'all' length scales

Geoffrey A. Ozin

Materials Chemistry Research Group, Chemistry Department, 80 St. George Street, University of Toronto, Toronto, Ontario, Canada M5S 3H6. E-mail: gozin@alchemy.chem.utoronto.ca

Received (in Cambridge, UK) 25th June 1999, Accepted 23rd August 1999

For the latter half of the 'Solid State 20th Century' materials science has been the engine that propelled technology. As we enter the 'Materials 21st Century' it is abundantly clear that the insatiable demand for new materials for emerging technologies is driving materials synthesis and change. Materials chemistry will play a central role in this endeavor through the creation of materials with structures and properties able to meet the demands required by up-and-coming technologies. In this paper a far-sighted and innovative materials chemistry strategy is proposed. It takes solid state chemistry beyond fifty years of thermodynamic phases and microscale structures, to a new era of self-assembly chemistry focused on metastable phases and mesoscale structures, with accessible surfaces and well defined interfaces that determine function and utility. It is an interdisciplinary approach that combines synthesis, solid state architecture and functional hierarchy to create an innovative strategy for materials chemistry in the new millennium. The attractive feature of the approach is the ability to assemble complex structures rationally from modular components and integrate them into self-assembling constructions for a range of perceived applications. By creating a series of purposeful design strategies it is believed that truly revolutionary advances in materials science and technology can result from this approach.

Room at the top and bottom

Not so long ago in materials chemistry it seemed that there was only 'room at the bottom'.[1] The trend was to synthesize and organize nanoscopic materials. As we enter the new millennium it is becoming abundantly clear that there is also 'room at the top'.[2] What has changed and why is this important? In this brief essay I will make the case that the paradigmatic shift comes from the realization that self-assembly, templating, patterning, capping, layering and molding methods have expanded the materials chemists tool box to include synthesis and organization of materials at 'all' length scales. Hierarchy has been introduced into materials chemistry and purely synthetic integrated chemical systems that are designed to achieve a particular function are becoming a reality. This augurs well for the development of materials, composites and systems with novel properties, new functions and perceived value in a range of applications in the biomedical, pharmaceutical, aerospace, automotive, construction, energy, electronics and photonics user sectors.

Self-assembling materials

This story is about interfaces between organics and inorganics and how they can be controlled synthetically at the molecular level to produce composite materials in which structure is prescribed from angstrom to centimeter length scales. The construction kit consists of complementary organics and inorganics that spontaneously assemble through lock-and-key intermolecular interactions. The driving forces for molecular organization are quite varied and as summarized in Scheme 1 can be based upon ionic, covalent, hydrogen, non-covalent, metal–ligand and colloidal bonding interactions, which may result in structures and properties not found in the individual components.

In this context, self-assembly may be viewed in terms of a map of bonding forces that operate between building blocks and over different length scales. In a self-organizing system, basic construction-units spontaneously associate to form a particular structure, the architecture of which is solely determined by the bonding properties and shapes of the individual components. The system proceeds towards a state of lower free energy and greater structural stability. Self-assembly is usually entropically driven in an aqueous system, where association of modules is accompanied by exclusion of ordered water molecules.

Hierarchy

A feature of self-assembly is hierarchy, where primary building blocks associate into more complex secondary structures that are integrated into the next size level in the hierarchy. This organizational scheme, which is illustrated in Scheme 2, continues until the highest level in the hierarchy is reached. These hierarchical constructions may exhibit unique properties that are not found in the individual components. Hierarchy is a characteristic of many self-assembling biological structures and is beginning to emerge as a hallmark of supramolecular materials. Self-assembly is considered to be distinct from template-directed assembly, which involves structure-directing additives, often organics or polymers, in addition to the constituent building-units, which may be inorganics. The

Geoffrey A. Ozin, born 23rd August 1943 in London, England, received his BSc degree in Chemistry from Kings College, University of London in 1965, and his DPhil degree in Inorganic Chemistry from Oriel College, Oxford University in 1967. He was an ICI Fellow at the University of Southampton from 1967–69 before joining the University of Toronto in 1969 where he is currently Professor of Chemistry. Recently he was a Canada Council Isaac Walton Killam Research Fellow and inducted into the Royal Society of Canada. He is a materials chemist and the current work of his group focuses on micro-, meso- and macro-structured materials and composites. The research exploits molecular recognition and self-assembly, to organize inorganic and organic building-units into materials with structural features that span angstrom to centimeter length scales. The methodology embraces concepts in supramolecular, host–guest inclusion, and biomimetic chemistry. Self-assembling mesostructures emerging from the research may find utility in areas such as electrically tunable membranes and chemical delivery systems, chemoselective sensors and solar cells, batteries and fuel cells, bone implants and photonics, nanocomposites and environmental clean-up of toxic waste.

DOI: 10.1039/a905090f

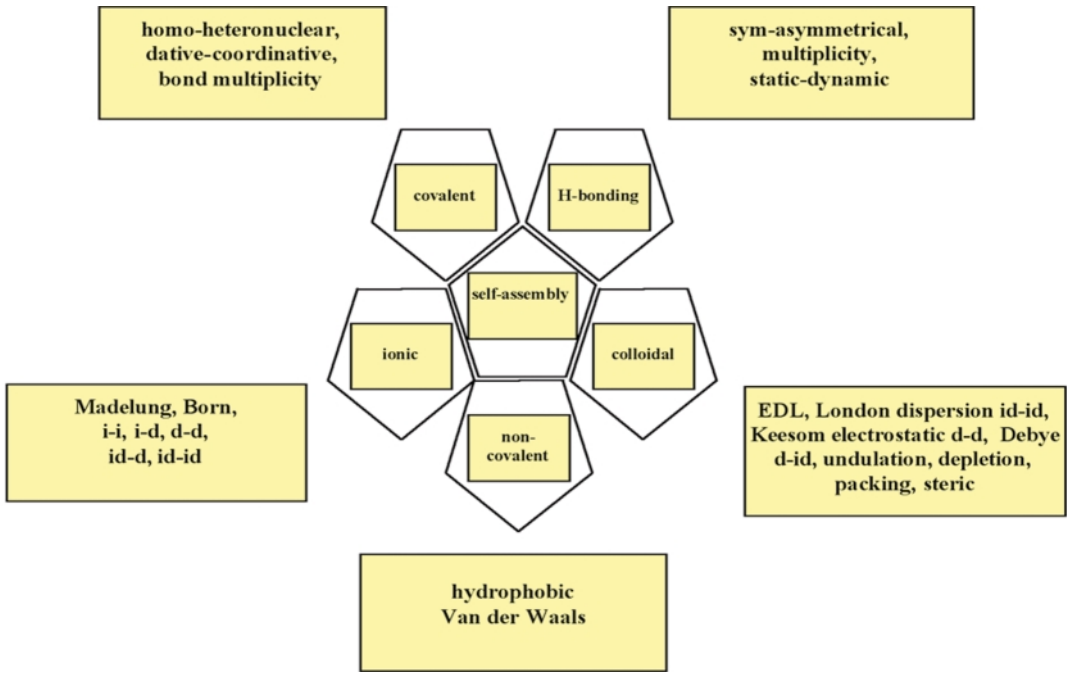

Scheme 1

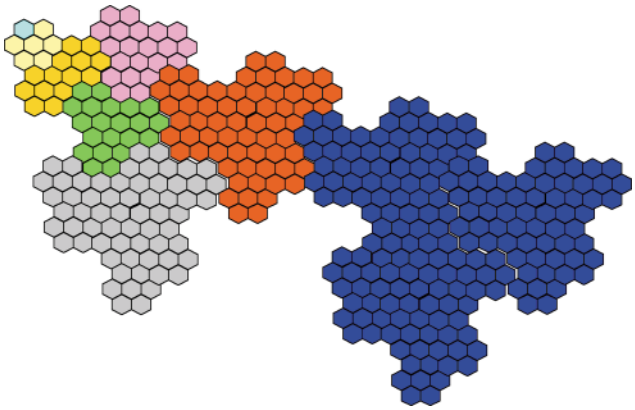

Scheme 2

template can serve to fill space, balance charge and direct the formation of a specific structure. In this definition, template assembly is synonymous with co-assembly and distinct from self-assembly.

Self-assembling materials over multiple length scales

Simple, elegant and robust attributes of self-assembly are now being combined with the powerful methods of inorganic and solid state chemistry to create supramolecular materials with unprecedented structures, compositions and morphologies. The paradigmatic shift of utilizing organics for templating,[3] capping,[4], layering,[5,6] wiring,[7] patterning[8] and molding[9] inorganics is having a revolutionary effect on the field of materials research. This is because it enables, for the first time, self-assembly of most elemental compositions of the periodic table but without the usual restriction of the dimension of structural components. This is facilitating purely synthetic approaches to hierarchical systems with the construction pieces integrated over micro-, meso- and macro-scopic length scales. This kind of 'panoscopic' synthesis, so to speak, has up until very recently been unparalleled in the field of solid state and materials chemistry. By combining the methodologies of self-assembly and microfabrication it has become feasible to assume the challenge of self-organizing and interconnecting functional organic, bio-organic, inorganic and polymeric chemical components into integrated electronic, photonic, mechanical, analytical and chemical systems for future 'panoscale' (panoscale: of any sizes, pano, L) devices.[10] Part of the motivation stems from the notion that the architecture of complex macrosystems in biology and engineering physics are generally based on hierarchical building principles, that is, smaller units are assembled into larger ones, which in turn are organized at a higher dimension. This construction process is continued until the highest level of structural complexity in the hierarchy has been attained.

The hallmark of an integrated chemical, physical or biological system is the assembly of components into a particular architecture that performs a certain function.[11] In the cell of a higher green plant the photosynthetic chloroplast and oxidative phosphorylation mitochondrion machines are perhaps two of the most impressive examples of functional integrated biological systems. Within the body of a computer the atoms are assembled into insulators, semiconductors and metals, dopants, junctions, metal leads and contacts. These are the building blocks that constitute the transistors, diodes and capacitors of the integrated circuits, which comprise circuit boards and subassemblies of an integrated microelectronic system. Familiar integrated chemical systems include heterogeneous catalysts, photoelectrochemical cells, solid state lithium batteries, hydrogen–oxygen fuel cells, instant color photographic film, sensors and chromatographic stationary phases.

The ability to self-assemble diverse kinds of materials over 'all' length scales and spatial dimensions has taken synthetic chemistry to a new level of structural complexity that begins to match those found in biology and engineering physics. It is now feasible to devise strategies for organizing, patterning and linking chemical components into functional architectures that were not previously accessible purely through synthesis. Representative examples taken from the recent literature include, layer-by-layer assembly of a thin film Zerner diode from conducting polymers and monodispersed capped semiconductor nanoclusters,[12] a metal–insulator–metal nanocluster–insulator–metal (MINIM) single electron transistor (SET),[13] a multicolor pixel voltage-controllable semiconductor cluster–luminescent polymer light emitting diode (LED)[14] an all-plastic field effect transistor driven light emitting diode (FET-LED),[15] and a high density rechargeable ultrathin graphite oxide

nanoplatelet–polyelectrolyte lithium ion battery.[16] These few examples serve to demonstrate the power and versatility of a self-assembly materials chemistry approach to 'panostructured' integrated chemical systems that perform a specific function.

'Panoscopic' synthesis can be viewed in terms of molecular level control of interfaces between organics and inorganics. As illustrated in Scheme 3, this allows one to embrace molecular,[17]

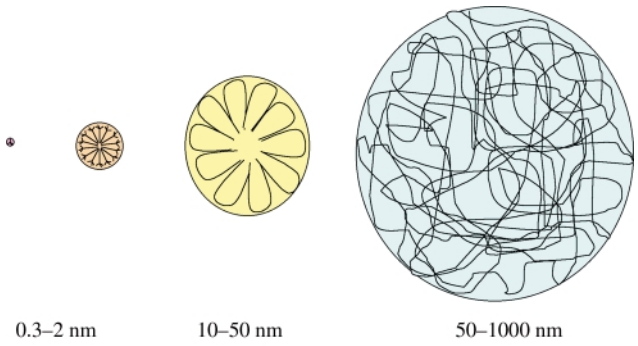

Scheme 3

supramolecular,[18] macromolecular,[19] and colloidal crystalline[20] assemblies under the umbrella of organic template-based assembly, facilitating the synthesis of inorganic materials over multiple length scales, with structural features that may span angstroms to microns.

Through a creative fusion of organic templating, inorganic chemistry, soft lithographic patterning and micromolding methodologies it is feasible to create functional hierarchical materials of the type sketched in Scheme 4. Entirely through

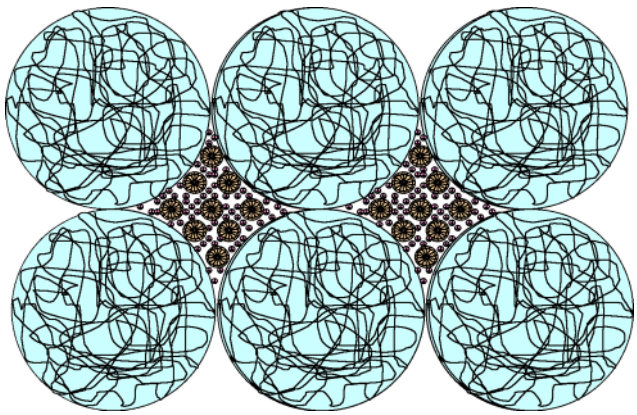

Scheme 4

chemistry one can plan how to synthesize, self-organize and interconnect different kinds of materials over 'all' length scales to create an integrated chemical system with single or multiple functions. In the following, I will briefly expand upon this theme by examining some case studies taken from our recent research to illustrate where 'panoscale' synthesis may find 'room at the bottom as well as the top' of the new materials world.

Faux diatoms and radiolaria

Interest in the synthesis of 'panascopic' materials may be traced to a report in 1995 of surfactant-templated mesolamellar aluminophosphates whose 'natural form' bore a striking resemblance to those of the lace-like siliceous microskeletons produced by the single cell marine organisms known as the diatoms and radiolarians.[21] When looking at scanning electron microscope (SEM) images of these purely synthetic forms it is sometimes difficult to distinguish them from the real thing, Fig. 1. This turned out to be the first synthesis that created a hybrid inorganic–organic material with a shape that mimicked an entire biomineralized skeleton found in the natural world.

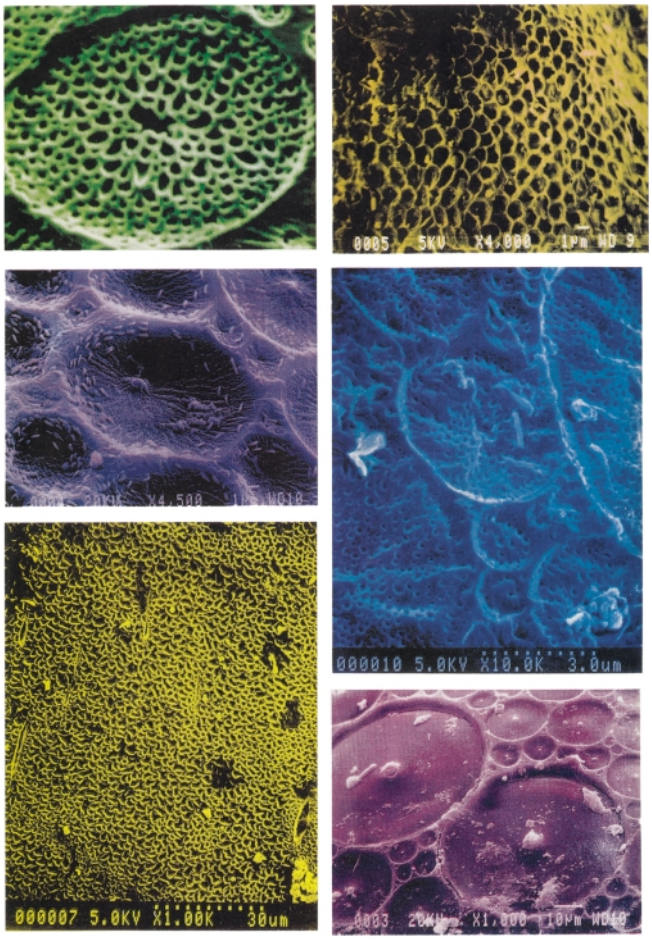

Fig. 1 Scanning electron micrograph images of synthetic examples of diatom and radiolarian microskeletons. Reprinted in part with permission from: *Adv. Mater.* (*London*) 1995, **7**, 943 (© 1995 Wiley-VCH) (top left, middle right); *Nature* (*London*) 1995, **378**, 47 (© 1995 Nature Publishing Group) (http://www.nature.com) (top right, middle left, bottom right); and *Acc. Chem. Res.* 1997, **30**, 22 (© 1997 American Chemical Society) (bottom left).

Fig. 2 Transmission electron microscopy image of the mesolamellar aluminophosphate material from which the synthetic diatoms and radiolaria mimics are built.

Multianalytical characterization of these synthetic natural forms revealed a hierarchical structure based upon a layered aluminophosphate.[21–25] The lamellae were well ordered at the mesoscale and glassy at the microscale, Fig. 2. Observed morphologies that emerged from a synthesis exhibited micron scale

patterns on millimeter sized solid and hollow spheres of a kind that are usually associated with the filigree microskeletons of diatoms and radiolaria. These aesthetically sculpted biological minerals continue to be admired in Ernst Haekel's *Art Forms in Nature*[26] and avidly read in D'Arcy Wentworth Thompson's *On Growth and Form*.[27]

How was such morphosynthesis possible in a laboratory setting? The template used to produce such shapes was dodecylamine, which in the presence of 85 wt% phosphoric acid formed dodecylammonium dihydrogen phosphate (DDP). Single crystal X-ray diffraction (SCXRD) established an interdigitated bilayer structure for DDP in which the ammonium head group was intricately hydrogen-bonded to the dihydrogen phosphate counter anion, Fig. 3. Powder X-ray diffraction (PXRD) and differential scanning calorimetry (DSC) showed that DDP transforms, under the reaction conditions that generate the patterned sphere shapes, to a thermotropic smectic liquid crystal phase. When observed between crossed-polarizers in a hot stage optical microscope (POM), as a film supported on a glass slide, the mesophase displayed the focal conic texture expected for a smectic liquid crystal,[22] Fig. 4. The optical birefringence pattern appeared even more pronounced when the DDP mesophase was formed in tetraethyleneglycol (TEG), which was the non-aqueous solvent used in the synthesis to create the patterned sphere shapes. The patterns seemed to be diagnostic of a microemulsion in which contiguous assemblies of phase separated water droplets were coated with a layer of the phosphate liquid crystal, Fig. 5. These observations suggested that the texture of the mesophase was 'fossilized' as a lamellar aluminophosphate by a POH + HOAl $\rightarrow$ P–O–Al + H_2O condensation–polymerization reaction of the dihydrogen phosphate anion with an aluminium(III) glycolate precursor located in the microphase separated domains of the DDP–TEG–H_2O liquid crystal microemulsion. This provided an appealing explanation for the origin of the micron-sized patterns observed on the surface of the mesolamellar aluminophosphate sphere shapes.

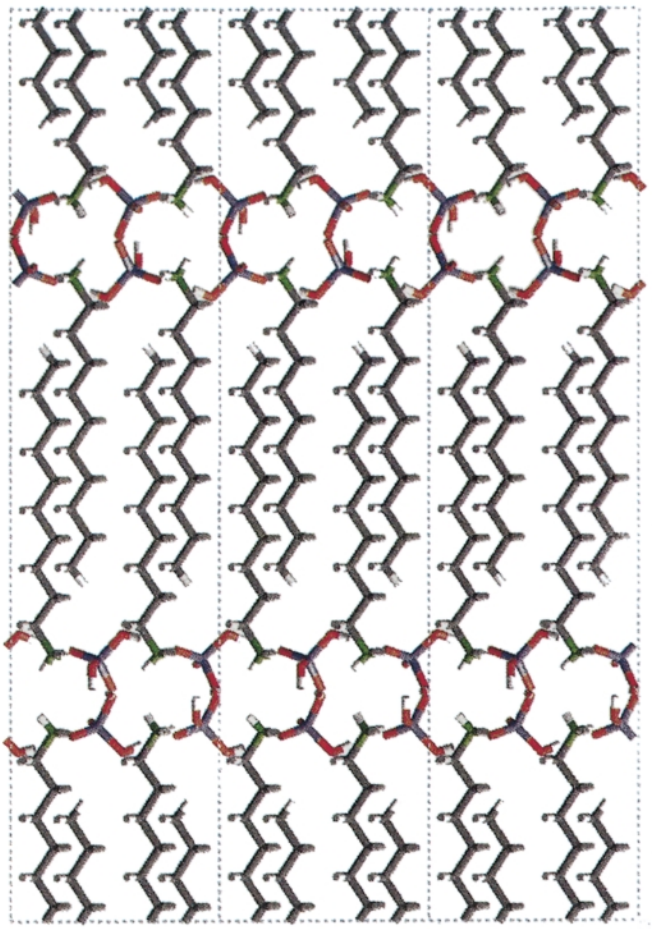

Fig. 3 Single crystal X-ray diffraction structure of dodecylammonium dihydrogen phosphate. Reprinted in part with permission from: *Acc. Chem. Res.* 1997, **30**, 24 (© 1997 American Chemical Society).

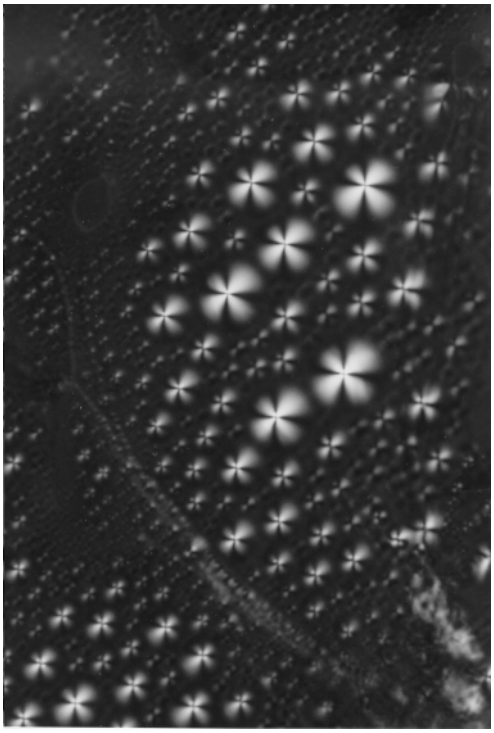

Fig. 4 Optical birefringence texture of smectic dodecylammonium dihydrogen phosphate mesophase.

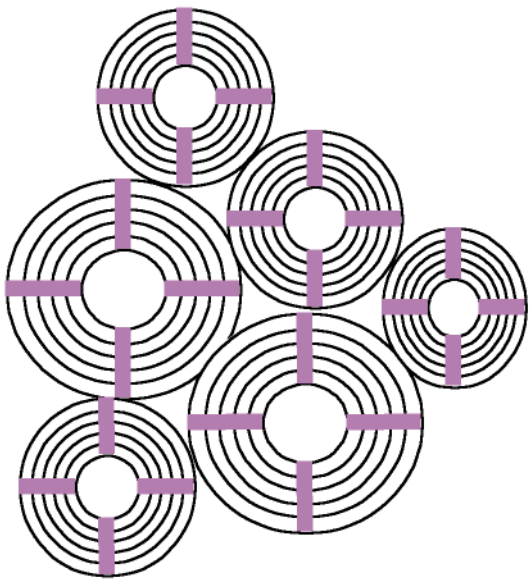

Fig. 5 Illustration of the smectic dodecylphosphate dihydrogen phosphate–tetraethyleneglycol–water liquid crystal microemulsion templating model for the morphogenesis of synthetic aluminophosphate diatom and radiolaria mimics.

It was the recognition that inorganic liquid crystals could be used to synthesize inorganic materials with complex form and structures spanning multiple length scales that raised the possibility of a purely synthetic approach to functional hierarchical materials such as bone mimics.

Synthetic bone implant materials

Synthetic analogues of bone are being actively pursued for biomedical applications in the field of bone replacement,

augmentation and repair.[28] Numerous stringent criteria have to be satisfied for a biomaterial to be acceptable as a bone implant, including the ability to integrate into bone and not cause any side effects. We recently described a biomimetic strategy to a new type of bone analogue material.[29,30] Bone consists of *ca.* 70% hydroxyapatite $Ca_{10}(PO_4)_6(OH)_2$, (OHAp), embedded in an organic matrix consisting mainly of the proteinaceous triple helix, collagen. Needle or plate-like morphologies of hydroxyapatite crystallize at regular intervals along the collagen fibers with the long *c*-axes oriented parallel to the fibrils. The presence of HPO_4^{2-} groups in bone apatites suggests that octacalcium phosphate $Ca_8(PO_4)_4(HPO_4)_2{\cdot}5H_2O$, (OCP), is a precursor to hydroxyapatite formation in bone. The OCP serves to establish the final morphology, composition, solubility and interfacial energy of apatitic materials, as well as controlling the nucleation and growth of OHAp. These result from the fact that OCP and OHAp have similar crystal structures and are able to epitaxially grow together.[31] A prime consideration in the preparation and performance of a bone implant material is the selection of a surface that is able to induce nucleation of OCP and growth of new bone.

With this background in mind we set out to synthesize an analogue of bone that comprised a porous hydroxyapatite–octacalcium phosphate–calcium dodecylphosphate (CDDP) composite film grown on a titania–titanium substrate. It has the hierarchical construction illustrated in Fig. 6. A macroporous

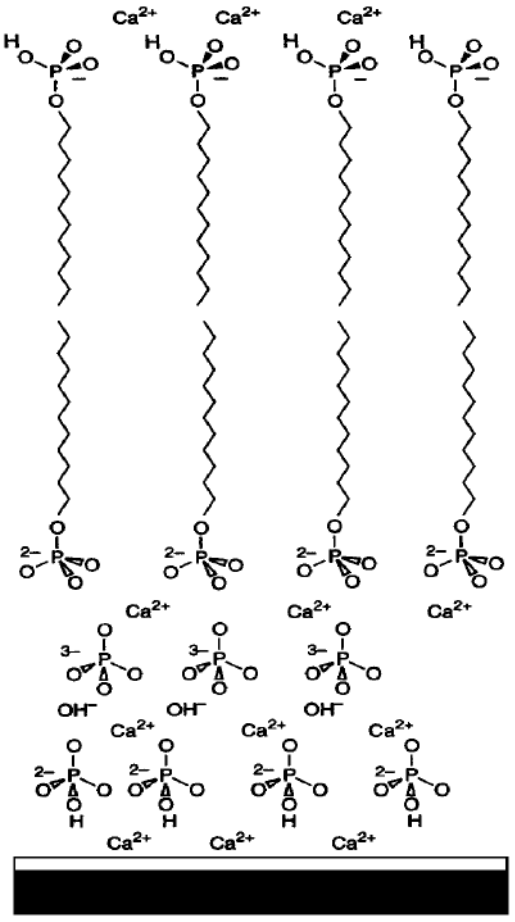

Fig. 6 Hierarchical construction of macroporous hydroxyapatite–octacalcium phosphate–calcium dodecylphosphate composite film grown on a titania–titanium substrate.

and oriented OHAp–OCP mineral phase was found to nucleate and grow, under physiological conditions, from TiOH Brønsted acid and base anchoring sites on the surface of a sputter-deposited titania film as seen in Fig. 7. The mesolamellar CaDDP phase was co-assembled with the OHAp phase in a 'mesoepitaxial' fashion as seen in Fig. 8. It is envisioned that if

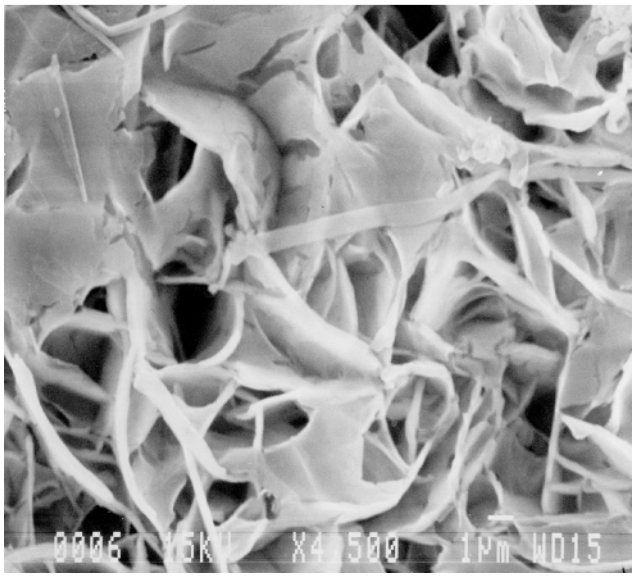

Fig. 7 Scanning electron microscopy image of macroporous hydroxyapatite–octacalcium phosphate–calcium dodecylphosphate composite film grown on a titania–titanium substrate.

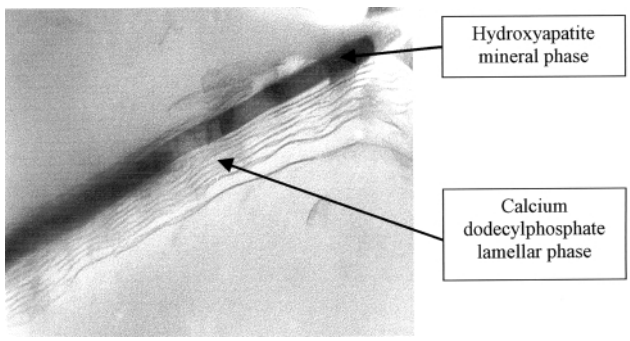

Fig. 8 Transmission electron microscopy image depicting the 'mesoepitaxial' relation between the calcium dodecylphosphate lamellar phase co-assembled with the hydroxyapatite mineral phase.

materials of this genre can integrate into bone they may be able to deliver bioeffectors and drugs, from the hydrophobic region of the CaDDP mesolamellar phase, to stimulate bone growth and combat disease. Notably, the macroporous structure of the material would facilitate the influx of cells and blood vessels to the site of the bone implant.

Tin sulfide mesh mesophase

The discovery of phosphate liquid crystals raised the possibility that other inorganic liquid crystals should exist and exhibit equally fascinating chemical and physical properties. Materials of this type are rare, they are anticipated to combine the fluidity of organic liquid crystals with for instance, the charge transport and optical properties of inorganic materials. This thinking led to the synthesis of a new class of tin sulfide liquid crystals with a novel structure based on a mesh mesophase.[32,33] The preparation involved the reaction of tin(IV) chloride with hexadecylamine and ammonium sulfide in aqueous ammonium hydroxide. The stoichiometry of the product, $HDA_{2{\cdot}67}SnS_{2{\cdot}05}$, suggested that the material had a structure with a very large void volume. In fact, it was found to have a structure based on regularly perforated layers of tin sulfide sandwiched between a bilayer of partially protonated and charge-balancing hexadecylamine. The room temperature phase was shown to be crystalline with well ordered inorganic and organic layers. The illustration depicts the structure of the as-synthesized crystalline tin(IV) sulfide mesoporous layers at room temperature (top), its semi-liquid crystalline form at 45 °C (middle) and its liquid

crystalline form at 85 °C (bottom), Fig. 9. Tapping mode atomic force microscopy (AFM) images of the material at room temperature revealed well ordered mesopores and mesola-

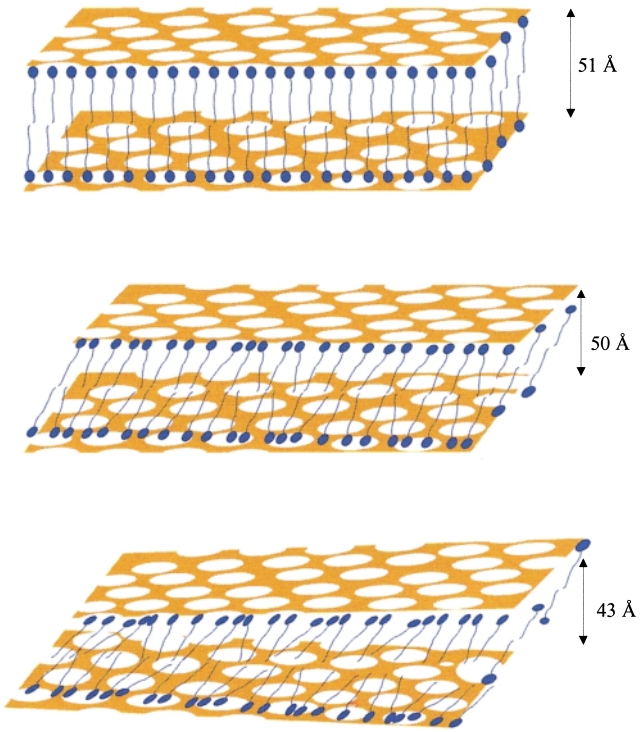

Fig. 9 Illustration of the structure of the tin sulfide mesh crystalline (top), semi-liquid crystalline (middle) and liquid crystalline (bottom) phase.

mellae, which was consistent with the results of powder X-ray diffraction (PXRD) and transmission electron microscopy (TEM), Fig. 10. The structure appeared to be best described as a tin sulfide replica of a mesh mesophase. A film of the room temperature crystalline phase had an electrical conductivity of 5.3×10^{-8} Ω^{-1} cm^{-1}. This increased by >1000 times on transforming to the liquid crystalline phase where it behaved as a semiconducting metallogen. Mesh type tin(IV) sulfide was found to be optically transparent and readily formed electrically conducting crystalline, semicrystalline or liquid crystalline thin films. Furthermore, it reversibly adsorbed molecules like H_2O and CO_2 with a concomitant and measurable electrical response. These observations bode well for the use of this new class of hybrid inorganic–organic semiconducting liquid crystals for display and chemical sensing applications.

Modular mesostructures

The work with tin sulfide liquid crystals suggested that metal sulfide cluster-based liquid crystals might be synthetically accessible and could provide a new and interesting way of assembling mesostructured metal sulfides from well defined building blocks. Earlier work involving the organic molecule templated assembly of adamantanoid $Ge_4S_{10}^{4-}$ clusters into crystalline microporous metal germanium sulfides showed that the integrity of the $Ge_4S_{10}^{4-}$ remained intact.[34] This suggested that cluster liquid crystals based on $Ge_4S_{10}^{4-}$ might be a good starting point to attempt the synthesis of mesostructured metal germanium sulfides. $TMA_4Ge_4S_{10}$ was readily accessible and could be ion exchanged for cationic surfactants like cetyltrimethylammonium chloride to form a lamellar germanium sulfide cluster mesophase $CTA_4Ge_4S_{10}$, Fig. 11. This appeared to be an attractive precursor for the assembly of mesostructured metal germanium sulfides, however the material was found to be insoluble in water, which prevented the formation of a lyotropic mesophase.

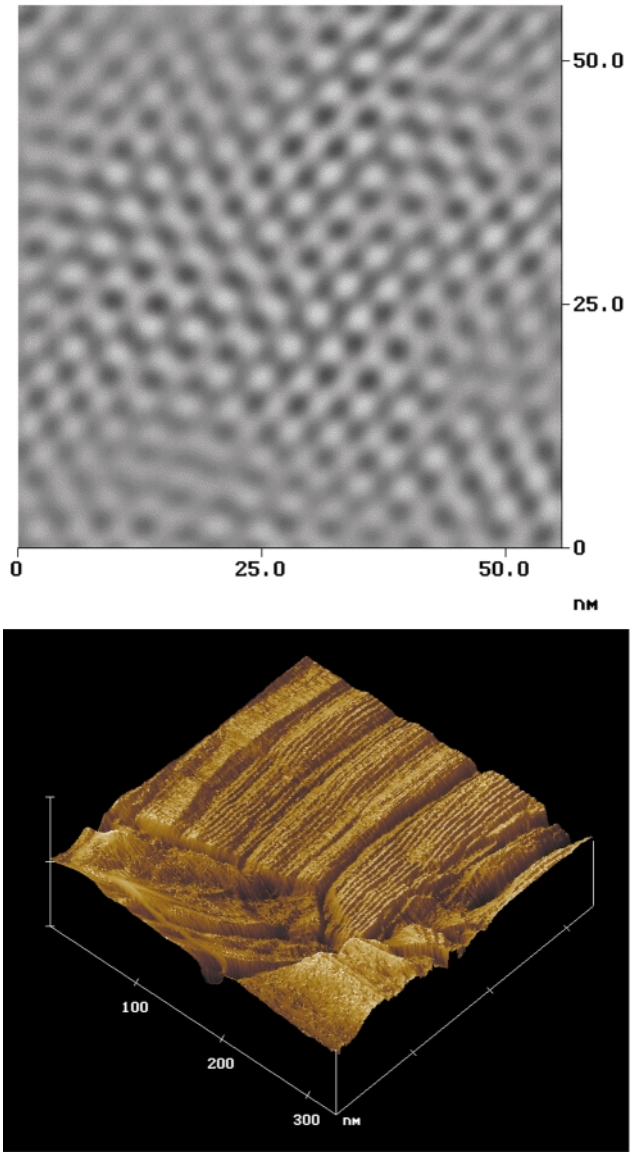

Fig. 10 Tapping mode atomic force microscopy images of the mesopores (top) and mesolamellae (bottom) in the crystalline tin sulfide mesh phase.

The solution to the problem, illustrated in Scheme 5, was found by using the interesting solvent formamide, $HCONH_2$, in which $CTA_4Ge_4S_{10}$ is soluble and self-assembles into a germanium cluster lyotropic liquid crystal.[35] Formamide is a strongly hydrogen-bonded solvent with a dielectric constant and boiling point higher than water. Moreover, the phase diagram of surfactants in formamide resembled that of surfactants in water. Using this knowledge it was discovered that adamantanoid $Ge_4S_{10}^{4-}$ clusters could be linked by divalent M^{2+} transition metal ions around a liquid crystal surfactant assembly in formamide to give exceptionally well ordered mesostructured metal germanium sulfide materials. Elemental analysis established the stoichiometry $CTA_2M_2Ge_4S_{10}$, which together with Raman spectroscopy of the precursor $CTA_4Ge_4S_{10}$ and microporous $TMA_2MGe_4S_{10}$ analogue proved that the cluster integrity remained intact, Fig. 12. These materials represented the first examples of 'coordination mesostructures', a new family of solids in which the $Ge_4S_{10}^{4-}$ cluster functions as a tetradentate ligand by coordinating through its four terminal sulfurs to transition metal ions like Co^{2+}, Ni^{2+}, Cu^{+}, Zn^{2+}.[35] By co-assembling the clusters and transition metal ions in this way, it proved possible to obtain a hexagonal mesostructure with metal linked adamantanoid clusters comprising the channel wall, Fig. 13. In the case of Cu^{+} compound the clusters were linked by Cu_2^{2+} dimers to create $CTA_2Cu_4Ge_4S_{10}$, an unusual example of a mesostructured material that contained a metal–

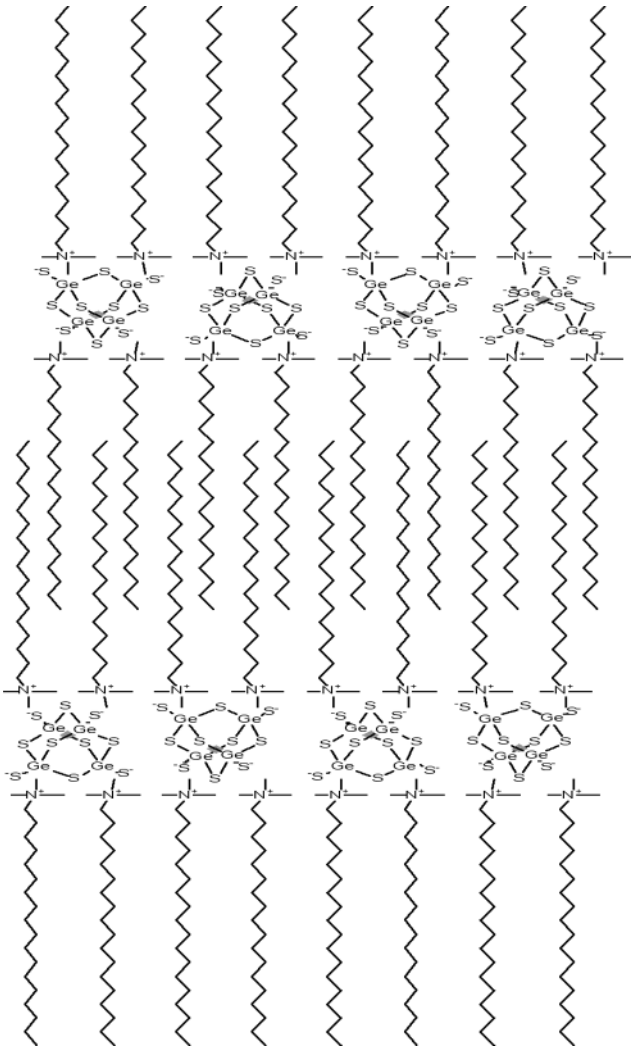

Fig. 11 Illustration of the lamellar adamantanoid germanium sulfide cluster crystalline phase.

metal bond like its microporous counterpart $TMA_2Cu_2Ge_4S_{10}$.[34,35] The supramolecular assembly of mesostructured materials from the linking of clusters was unprecedented. From consideration of the architecture and composition of mesostructured metal sulfide materials it is envisioned that they could prove effective in diverse applications, such as detoxification of heavy metals in polluted water streams, sensing of sulfurous vapors and semiconductor quantum anti-dot devices.

Sol–Gel mesophase

Continuing with the theme of inorganic liquid crystals that can mineralize into mesostructured inorganic replicas of the templating mesosphase, raised the possibility that a generalized non-aqueous synthesis of main group and transition metal oxide mesostructures could be developed based upon the hydrolytic condensation–polymerization of a sol–gel mesophase. This led to the discovery of glycosilicate and glycometallate surfactants that self-assemble into a hydrolyzable lamellar mesophase.[36,37] The surfactant was cationic and the glycometallate functioned as the charge compensating counter anion, Fig. 14. The main advantage of hydrolyzable glycometallate surfactants was found to be the control that could be exerted over the condensation–polymerization of source reagents like silicates, titanates, zirconates and niobates. This proved pivotal to the successful incorporation of two or more metals into the framework of binary or ternary mesoporous metal oxide materials. Glycometallate precursors may be considered as

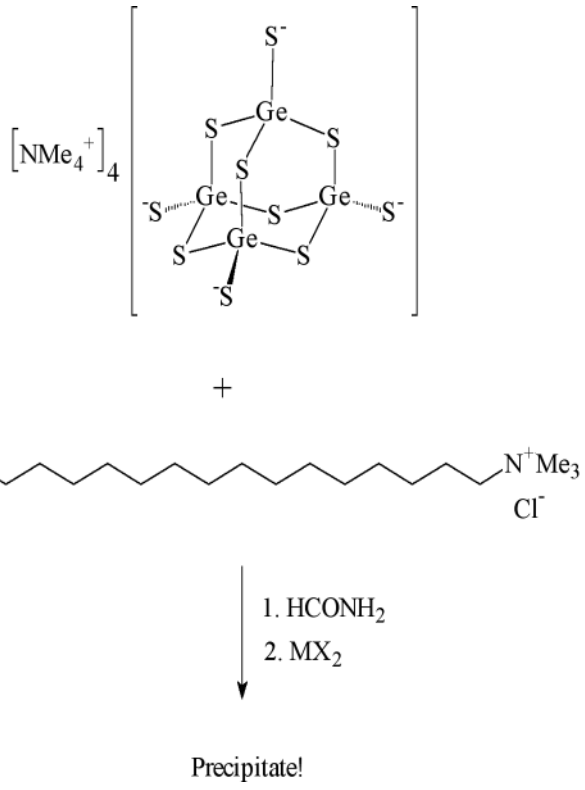

Scheme 5

bidentate metal alkoxides. They provide better command over differential rates of hydrolysis of binary combinations compared to traditional monodentate metal alkoxides or bulk metal oxide source materials.

Hydrolysis of Si(IV), Ti(IV), Zr(IV) and Nb(V) glycometallates was found to produce well-ordered mesoporous metal oxides, Fig. 15. Following treatment with metal alkoxides or disilane coupling reagents the surfactant template could be removed to create high surface area narrow pore size distribution mesoporous binary metal oxides. The glycosilicate mesophase showed a well defined lamellar to hexagonal structural transition, which appeared to originate from polymerization induced size and charge density changes in the headgroup region of surfactant. Binary silica–transition metal oxide, mesoporous materials that are rich in either the silica or metal component have been synthesized from a mesophase comprised of mixed glycometallates.

Glycometallate surfactants provide a facile synthetic entry to electroactive and photoactive mesoporous metal oxide materials. They are anticipated to function as electrodes, electrolytes and plasticisers in solid state batteries, fuel cells, solar energy conversion devices, and large molecule chemical sensors.

Mesostructured solid electrolytes

Inorganic liquid crystals again played a central role in the synthesis of a new class of solid electrolytes coined 'salted mesostructures'.[38] In a one-pot synthesis, a lithium triflate–silicate–oligo(ethylene oxide) surfactant mesophase was found to undergo an acid catalyzed polymerization to generate a lithium triflate–oligo(ethylene oxide) surfactant–mesoporous silica nanocomposite film. The optical birefringence fan texture observed for the film was that expected for a silicified version of the hexagonal symmetry mesophase, Fig. 16. $LiCF_3SO_3$ was found, by NMR and Raman spectroscopy, to be dissociated into free lithium (small solid black circle) and triflate (large hatched circle) ions, which were contained in the oligo(ethylene oxide) head group region of the surfactant assembly (thin black lines), all imbibed within the channels (thick black line) of the

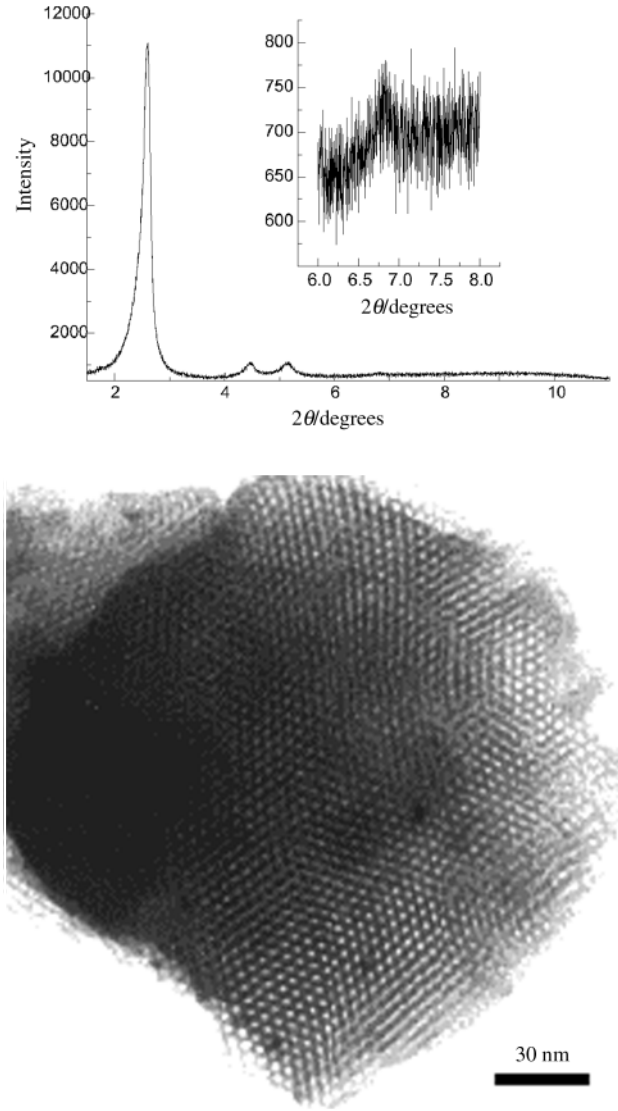

Fig. 12 Powder X-ray diffraction pattern (observed d_{hkl} = 100, 110, 200, 210) and transmission electron microscopy image of the hexagonal form of mesostructured nickel (top) and cobalt germanium sulfide (bottom).

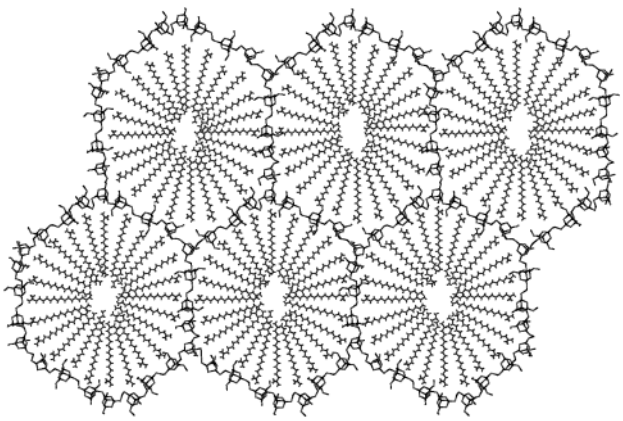

Fig. 13 Illustration of the structure of hexagonal symmetry mesostructured metal germanium sulfide assembled from metal linked adamantanoid germanium sulfide clusters around a surfactant mesophase.

mesoporous silica, Fig. 17. Nanocomposite materials of this genre have been found by ac impedance spectroscopy to behave as fast lithium ion conductors at room temperature, which bodes well for them finding utility in the important field of polymer electrolyte, plasticiser and battery technology.

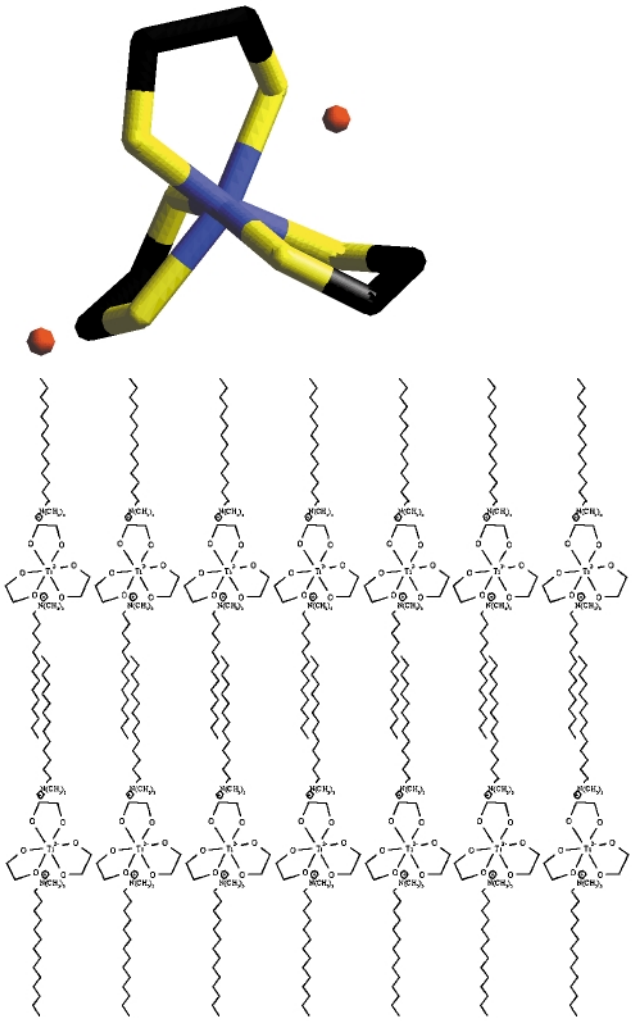

Fig. 14 Illustration of sodium glycotitanate(IV) (top) and lamellar cetyltrimethylammonium glycotitanate(IV) mesophase (bottom).

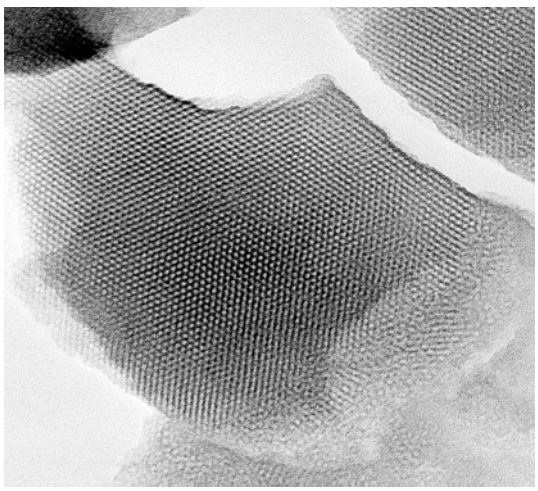

Fig. 15 Transmission electron microscopy image of mesosporous zirconia assembled from glycozirconate around a surfactant mesophase.

Polymer–mesoporous silica nanocomposites

The ability to control the morphology and mesostructure of surfactant-templated silica as fibers, films, spheres, gyroids, discoids, spirals and soft lithographically defined micron scale patterns depends on the integration of chemical and physical concepts in surfactant, sol–gel, liquid crystal, surface, colloid and crystal growth science.[39,40] This entailed command over topological defects, director fields, surface charge, nucleation

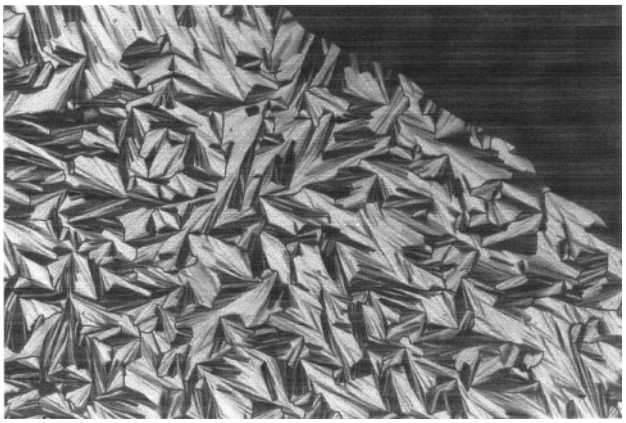

Fig. 16 Optical birefringence texture of lithium triflate–oligo(ethylene oxide) surfactant–mesoporous silica composite film.

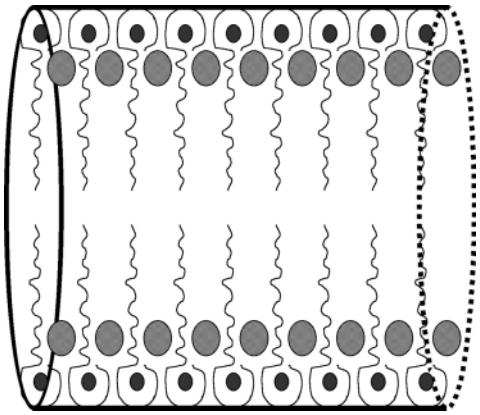

Fig. 17 Illustration of the channel architecture of lithium triflate–oligo(ethylene oxide) surfactant–mesoporous silica composite film.

and growth of polymerizable silicate micelles and liquid crystals. The availability of shaped forms of hexagonal mesoporous silica, like those illustrated in Scheme 6, raised the interesting possibility of using host–guest inclusion chemistry to synthesize a range of nanocomposites, nanowires and nanoclusters, which may possess unique electrical, optical and mechanical properties. Spatially self-limiting synthesis of this genre has enabled the production of polymer nanocomposites. Subsequent etching of the silica host was able to provide a route to polymer mesofibres with the same diameter as the channels of the host.

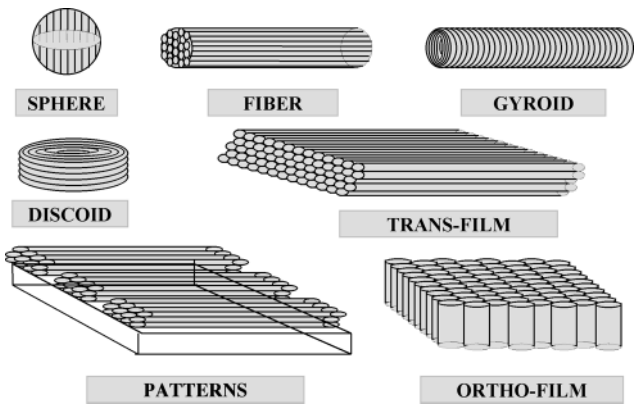

Scheme 6

To amplify, phenol and formaldehyde were introduced into the channels of hexagonal mesoporous silica. Exposure to gaseous hydrogen chloride induced a condensation polymerization of the monomer precursors in the channels to form a cross linked poly(phenolformaldehyde)–mesoporous silica nanocomposite material.[41] Proof for the formation of intrachannel poly(phenolformaldehyde) in mesoporous silica was obtained by TEM imaging of aqueous HF extracted fibers. They were found to have a diameter of *ca.* 20–30 Å and aspect ratios as high as 10^4, Fig. 18. Depending on the details of the HF extraction process the polymer could be formed as either individual strands or bundles of fibers.

Fig. 18 Transmission electron microscopy image of poly(phenolformaldehyde) mesofibers extracted from poly(phenolformaldehyde)–mesoporous silica composite. Scale bar = 10 nm.

Inorganic polymer–mesoporous silica nanocomposites

This paradigm has been effectively used to synthesize a poly(ferrocenylsilane)–mesoporous silica composite, Fig. 19, by the ring opening polymerization of a silaferrocenophane within the channels of hexagonal mesoporous silica.[42] Temperature controlled heating in the range 500–1000 °C caused the encapsulated polymer fibers to pyrolyze and form a well ordered, superparamagnetic ceramic–silica nanocomposite, Fig. 20. The composite materials were shown to contain monodisperse superparamagnetic iron nanoparticles embedded in a SiC/C matrix, housed within the channels of the mesoporous silica host.

Silicon–silica nanocomposite film

Work of a related kind concerns the synthesis of silicon nanoclusters in hexagonal mesoporous silica film that displays bright visible photoluminescence and nanosecond lifetimes.[43] This is notably distinct to the longer millisecond and microsecond emission lifetimes usually observed for nanocrystalline and bulk forms of silicon.[44–46] The process of creating the luminescent silicon–silica nanocomposite film is purely synthetic and works well under very mild conditions. It is simple to execute, low cost, may be integrated into existing silicon technology and could be suitable for mass production. The methodology may be useful for the fabrication of silicon-based light emitting diodes, optical interconnections, displays and chemical sensors.

To amplify, chemical vapor deposition (CVD) of disilane Si_2H_6 at 140 °C and 30 Torr in free standing, oriented hexagonal mesoporous silica film, yielded photoluminescent silicon nanoclusters. This mild CVD process necessitated the use of an incompletely polymerized mesoporous silica film that contained a high population of hydroxy SiOH wall sites as well as

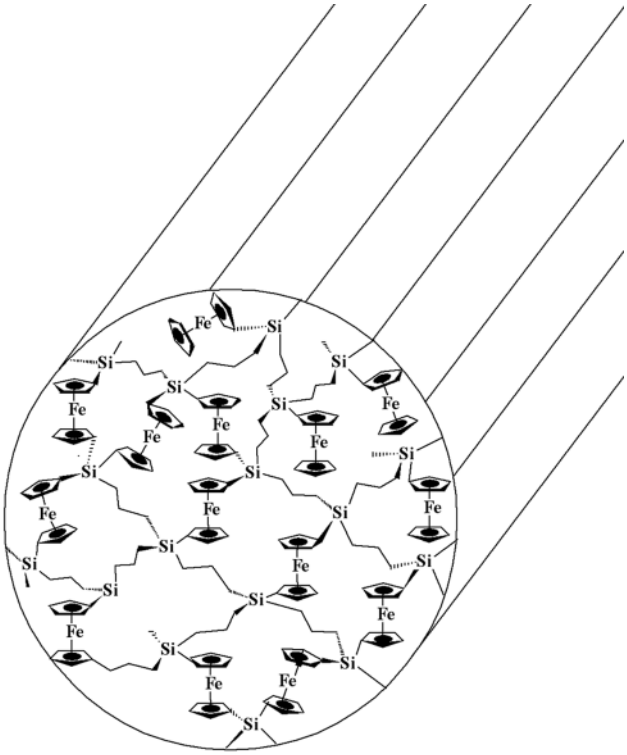

Fig. 19 Illustration of channel architecture of poly(ferrocenylsilane)–mesoporous silica composite.

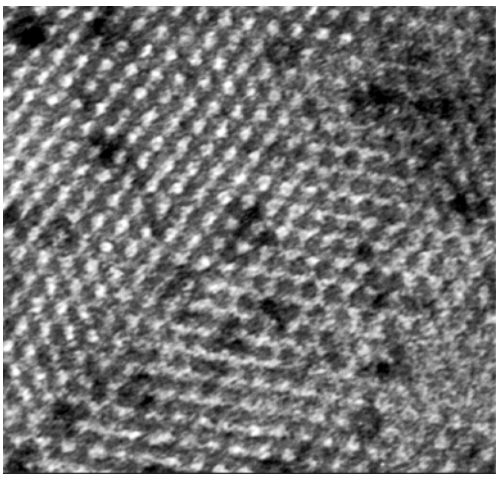

Fig. 20 Transmission electron microscopy image of superparamagnetic iron clusters in a silicon carbide–carbon matrix housed within the channels of a mesoporous silica host.

the surfactant template, required to make the film, within the channels. Exposure of the film to gaseous Si_2H_6 led to a silicon–silica nanocomposite film that displayed bright luminescence in the visible spectrum. Adsorption of Si_2H_6 into the film appeared to be facilitated by the surfactant imbibed within the channels. Anchoring of Si_2H_6 in the film occured at reactive SiOH sites located in the silica channel wall. Thermally induced hydrogen-elimination from anchored $Si_2H_6 \cdots SiOH$ and aggregation of silicon proceeded in the channel spaces of the film. This process restricted the growth of silicon clusters to the dimensions of the mesoscale channels. Raman, solid state NMR and luminescence spectroscopic techniques indicated that the size of the encapsulated silicon nanoclusters was *ca.* 1–2 nm and in this range they exhibited distinct structural and electronic properties compared to larger silicon nanocrystallites and bulk silicon, Fig. 21. This is believed to be the origin of the observed nanosecond lifetimes of the photoluminescence from the silicon–silica nanocomposite film.

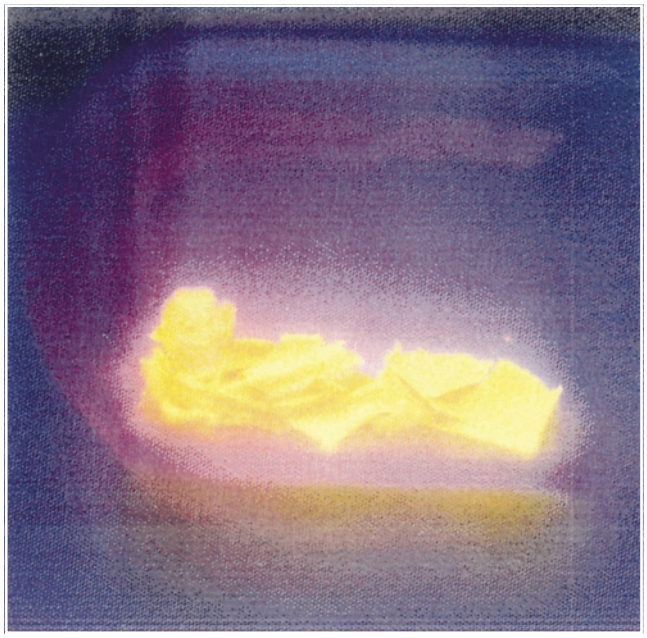

Fig. 21 Photoluminescence from 1–2 nm diameter silicon nanoclusters housed within the channels of hexagonal mesoporous silica film.

Buckling silicate liquid crystals

Morphosynthetic control of the nucleation, growth and polymerization of a lyotropic silicate liquid crystal has enabled sculpting of fiber, film and sphere shapes out of hexagonal mesoporous silica.[39,40] While topological defects (*e.g.* disclinations and dislocations) and colloidal interactions (*e.g.* electrical double layer, van der Waals) play a dominant role in the genesis of a particular form of mesoporous silica, more subtle elastic and compressive forces have been found to be responsible for the creation of radial patterns and twisted shapes like those shown in Fig. 22.

Patterning

Intriguing designs have been found on the surface of mesoporous silica shapes.[47] Radial patterns observed on discoid morphologies are particularly impressive, as judged by Fig. 23. While the relation between bulk and surface mesostructure, optical birefringence and morphology provided a useful insight into morphogenesis of curved mesoporous silica shapes, the origin of surface patterns remained an enigma and a challenge for materials chemistry. Analysis of the radial patterns of a large number of discoids showed the nodal frequency spans from zero to over a hundred with no obvious trend in the observed values. To gain an insight into the morphogenesis of radial patterns in mesoporous silica discoid shapes, the theory of elasticity for nematics with some modification was considered a logical starting point. The equilibrium shape of a hexagonal silicate mesophase confined to a regular discoid geometry (concentric co-axial director field, 2π line disclination) was obtained by integrating the free energy density over the volume of the liquid crystal, taking into account the surface tension term. It was found that the minimum energy of a regular discoid mesophase is attained by an elastic deformation to create a discoid with a radial pattern that was similar to those observed on mesoporous silica discoid shapes.

Although calculations predicted that radial patterns could appear on a planar discoid, it was found experimentally that radial patterns often occur on corrugated and/or sunken discoid shapes, Fig. 23. Clearly, some other distortion was operative in the silicate discoid mesophase besides just spontaneous elastic deformation and that had not been taken into account in the free energy calculations. The missing contribution to the growth process was believed to originate from longitudinal and radial

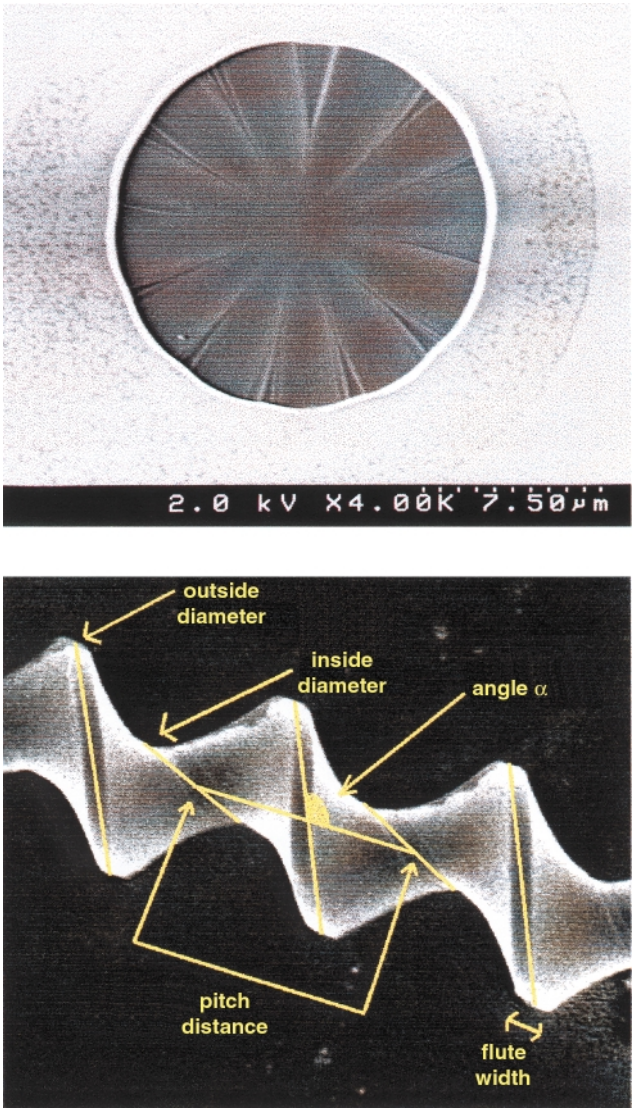

Fig. 22 Scanning electron microscope images of radially patterned discoid (top) and of hollow Archimedian screw (bottom) shapes both made of hexagonal mesoporous silica.

differential contraction of micelle rods that comprised the liquid crystal discoid and that was induced by polymerization of silicate to silica. Because growth of a discoid was imagined to occur from the center and radially outwards, the inner portion of the discoid was expected to be more polymerized than the outer region. The outcome of including polymerization induced differential contraction effects into the calculation of the shape of the radially patterned mesoporous silica discoid was to create sunken discoid shapes like those shown in Fig. 23.

Supramolecular origami

Similar kinds of polymerization induced differential contraction but now confined to a patch of hexagonal mesoporous silica film were found to be responsible for the morphogenesis of hollow helicoids of mesoporous silica.[48] It was found that a low acidity and high ionic strength medium favored a slow rate of silicification in a patch of mesoporous silica film. Hence polymerization-induced differential contraction of silicate micelle rods became influential in the formation of hollow helicoids rather than the formation of a mesoporous silica film. PXRD clearly defined the materials as hexagonal mesoporous silica and SEM images revealed shapes that resembled an Archimedian screw, Fig. 22. TEM images recorded for whole-mounted helicoids revealed that they were hollow with *ca.* 1 μm thick 'shell'. The shell was found to be composed of

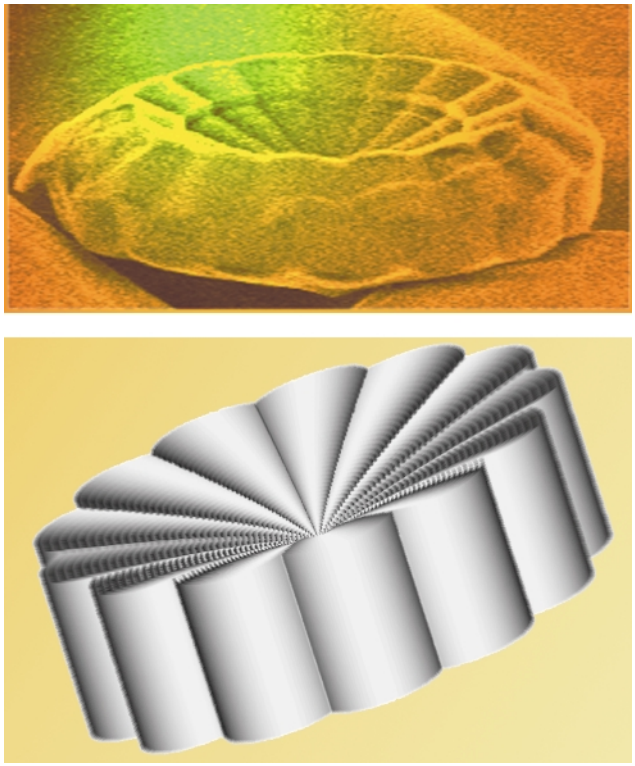

Fig. 23 Observed and calculated sunken and radially patterned hexagonal mesoporous silica discoid.

hexagonally close-packed *ca.* 5 nm diameter channels, which had a *ca.* 1 nm thick silica wall and appeared to spiral around the major axis of the helicoid. The dimensions of a significant collection of hollow helicoids were analyzed by measurements of SEM images. It was striking that diagnostic dimensions of the screw, namely pitch width and angle, flute width, and inside and outside diameter, were found to span a rather narrow range. Notably, the pitch angle α was centered at 70 and 110°, which, respectively, corresponded to left and right handed helices that occurred in essentially equal numbers within the same synthesis batch. From the collective evidence it was concluded that hollow helical cylinders originated from polymerization induced differential contraction of a hexagonal silicate liquid crystal 'patch', which contracted further into hollow helicoids made of hexagonal mesoporous silica, Fig. 24.

The folding mechanism illustrated in Fig. 24 is based upon both radial and longitudinal contractions across and parallel to the rods/channels, respectively, induced by polymerization of a hexagonal silicate mesophase to mesoporous silica. As the patch grows in area and thickness, older rods must undergo more polymerization and contraction than younger ones. Provided radial and longitudinal differential contractions in thickness are considered, they lead to diagonal bending of the patch because these two contractions act in mutually orthogonal directions. Within this diagonally folded patch, the volume of the micelle rods changes solely by contraction but not deformation. Therefore, the folded patch is stress-free, that is in an energetically favorable configuration.

Synthetic shape

The understanding that emerged from these studies has revealed new ways of controlling the growth and form of composite inorganic–organic mesostructured materials with novel topologies. Siliceous hollow helicoids with spiraling channels may find utility for separating viral or bacterial particles, in the synthesis of chiral macromolecules, and as micromolds for the fabrication of magnetically activated screws in microelectromechanical, microfluidic and microanalytical devices. The ability to intentionally synthesize micron-sized shaped objects

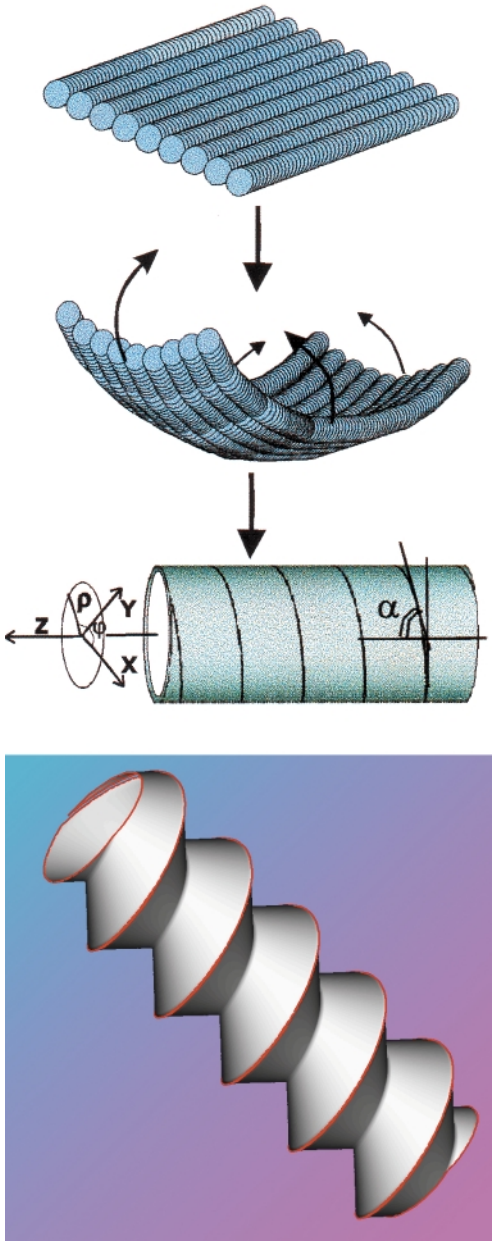

Fig. 24 Supramolecular origami: polymerization induced differential contraction and folding of a patch of hexagonal silicate liquid crystal film to give a mesoporous silica hollow cylinder (top) which further contracts to a hollow helicoid (bottom).

begins to point the way to self-assembling 'synthetic' micro-electro-mechanical machines (SMEMS), like the one imagined in Fig. 25. One might be able to employ this approach as an alternative or adjunct to currently employed MEMS techniques, which rely on the fabrication of components. This paradigm raises some intriguing possibilities for future 'panoscale' research aimed at the organization and integration of synthetically shaped materials for functional devices.

New nanocomposites: a fusion of synthetic organic and solid state materials chemistry

A brand new class of self-assembling nanocomposite materials called periodic mesoporous organosilica materials (PMOs) has recently been discovered.[49–53] What is so special about these nanocomposites is that for the first time organic functionality has been chemically integrated 'within' the framework of a solid state inorganic structure.

These organic–inorganic hybrids are prepared through the surfactant-templated hydrolytic polycondensation of bis(triethoxysilyl)organo precursors, $(EtO)_3SiRSi(OEt)_3$, in which

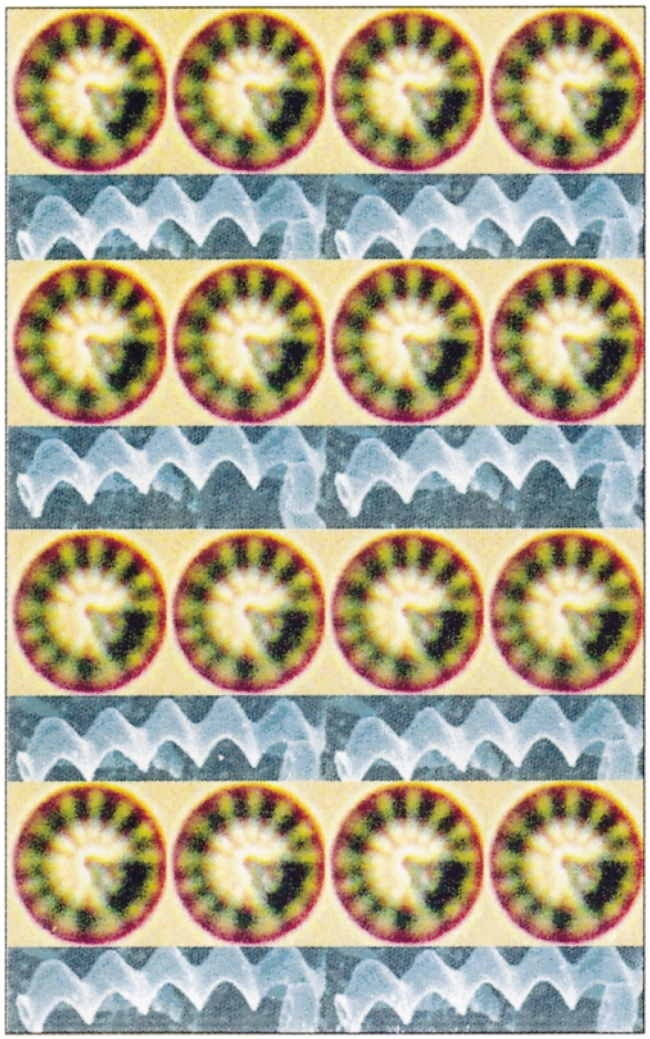

Fig. 25 Concept of futuristic synthetic microelectromechanical machines, SMEMS.

two sol–gel moieties are connected by an organic group R. Bridging organic groups that have been successfully integrated into the silica framework include ethane, ethene, methylene, benzene, thiophene, ferrocene and acetylene.[49–53] Significantly, the methodology also enables the synthesis of controlled morphology PMOs in the form of optically transparent monoliths and films (see Fig. 26).[54] This approach extends the realm of periodic mesoporous materials to 'chemistry of the channel walls' rather than limiting the 'chemistry to the channel space', which had been the situation until these reports.

The synthesis of PMOs fuses methodologies in organic synthesis, sol–gel chemistry and supramolecular assembly, to create a new class of nanocomposites in which the interface between the organic and inorganic components is under molecular scale control. What is so appealing about PMOs is the 'designed integration' of organic functionality 'inside' the actual framework of a solid state inorganic material, which exhibits crystalline mesoporosity. This is considered a breakthrough for several reasons. It allows the composition, hydrophobicity–hydrophilicity, and chemical properties of the mesoporous host to be tuned using chemistry. There is potential to chemically change the mesoporous material to modify the physical and mechanical properties of the mesoporous host—no other material designed thus far can claim this possibility. The functional groups do not hinder space inside the channels, as do terminally grafted organic groups. It permits a greater fraction (100% loading) of organic species to be placed in the framework of the material than other synthetic routes, which put organic groups inside the channel voids and are restricted to 25% loading before all order is lost. Also, it ensures a

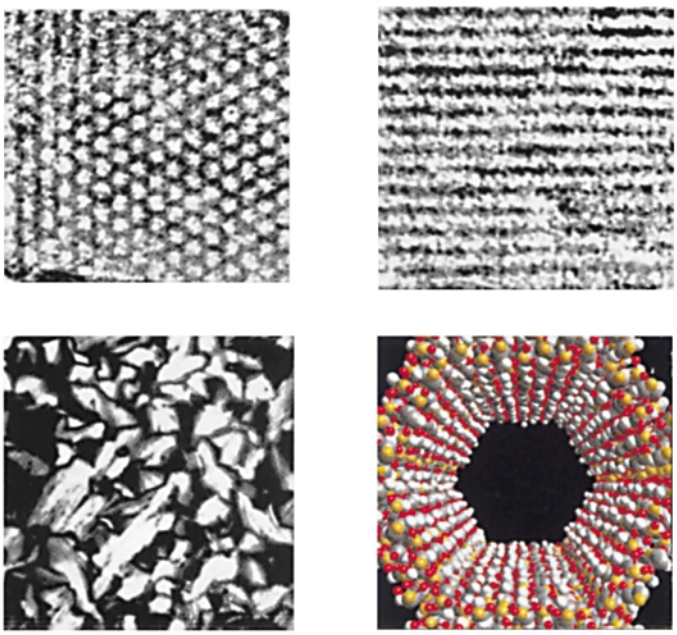

Fig. 26 Transmission electron micrograph (top left and right) and polarization optical microscope (bottom left) images and graphical representation of a single channel (bottom right) of optically transparent oriented hexagonal mesoporous ethenesilica film.[54]

homogeneous distribution of organic groups inside the walls of the materials.

Having reactive organic groups chemically integrated 'inside' the channel wall of periodic mesoporous silicas, rather than simply grafted to and hanging in the channel spaces, may prove to be advantageous for many applications. Moreover, there are additional advantages that may arise from the incorporation of organics into the 'backbone' of the material. Owing to the flexibility of organic spacers, PMO film and monolithic samples may be less prone to cracking, a problem that has always plagued research involving controlled morphology mesoporous silica materials. Moreover, the hardness and density of the bulk mesoporous organosilica may be tuned by changing the organic groups. This provides a new route to lightweight periodic mesoporous materials. Clearly, many opportunities abound for periodic mesoporous organosilicas with appropriately designed functional organics 'inside' the framework.

Value of panoscopic materials

Ultimately, the scientific and technological impact of any new class of materials depends on the ability to control the size, morphology and aggregate structure of primary particles. Self-assembling 'panoscopic' materials are no exception in this respect. They introduce hierarchy into materials chemistry and bode well for the development of materials and composites with novel properties, new functions and perceived utility in a range of applications in the biomedical, pharmaceutical, aerospace, automotive, construction, energy, electronics and photonics sectors. Possibilities for 'panostructured' materials include large molecule catalysis, membrane separation and sensing, battery electrolytes, low dielectric electronics packaging, chiral separation stationary phases, bone implants, chemical delivery vehicles, and toxic clean-up of water streams, The future looks very bright for self-assembling 'panoscopic' materials.

Acknowledgements

The research described in this personal account has profoundly influenced my way of thinking about materials chemistry. Chemical concepts in self-assembly, length scales, hierarchy, integration and topology have been introduced that hopefully will make a difference to the way materials research evolves in the new millennium. None of this would have been possible without the contributions of my talented coworkers whose names are listed in the references and who challenged me every day with important, insightful and creative ideas and suggestions. Dr Charles Kresge of Mobil, Dr Robert Bedard of UOP and Dr Juan Garces of Dow have championed the research in the U of T materials chemistry group for many years and were regular visitors in Toronto for many memorable brainstorming sessions, both in the laboratory and at great restaurants. During this exciting period of research, G. A. O. was awarded an Isaac Walton Killam Memorial Fellowship from the Canada Council. G. A. O. is also grateful to the Natural Sciences and Engineering Research Council (NSERC) of Canada for financial support of this work. Support and encouragement from the Chairman of the chemistry department, Dr Martin Moskovits, is appreciated. And last but not least I wish to express my gratitude to my best friend Linda Ozin who tries to make my writing more lucid.

References

1 R. Feynmann, *Sci. Eng.*, 1960, **23**, 22; G. A. Ozin, *Adv. Mater.*, 1992, **4**, 612.
2 G. A. Ozin, E. Chomski, D. Khushalani and M. MacLachlan, *Curr. Opin. Coll. Surf. Sci*, 1998, **3**, 181; S. Mann and G. A. Ozin, *Nature*, 1996, **382**, 313.
3 C. T. Kresge, M. Leonowicz, W. J. Roth, J. C. Vartuli and J. C. Beck, *Nature*, 1992, **359**, 710.
4 R. L. Whetten, M. N. Shafigullin, J. T. Khoury, T. G. Schaaff, I. Vezmar, M. M. Alvarez and A. Wilkinson, *Acc. Chem. Res.*, 1999, **32**, 397.
5 G. Decher, *Science*, 1997, **277**, 1232.
6 S. W. Keller, H. N. Kim and T. E. Mallouk, *J. Am. Chem. Soc.*, 1994, **116**, 8817.
7 R. C. Mucic, J. J. Storhoff, C. A. Mirkin and R. L. Letsinger, *J. Am. Chem. Soc.*, 1998, **120**, 12674.
8 Y. Xia and G. M. Whitesides, *Angew. Chem., Int. Ed.*, 1998, **37**, 550.
9 C. R. Martin, *Science*, 1994, **266**, 1961.
10 G. M. Whitesides, *Sci. Am.*, 1995, **273**, 146.
11 *Integrated Chemical Systems, A Chemical Approach to Nanotechnology*, ed. A. J. Bard, John Wiley and Sons, Inc., New York, 1994.
12 T. Cassagneau, T. E. Mallouk and J. H. Fendler, *J. Am. Chem. Soc.*, 1998, **120**, 7848.
13 D. L. Feldheim, K. C. Grabar, M. J. Natan and T. E. Mallouk, *J. Am. Chem. Soc.*, 1996, **118**, 7640.
14 J. E. Bowen Katari, V. L. Colvin and P. Alivasatos, in *Biomimetic Materials Chemistry*, ed. S. Mann, VCH, New York, 1996.
15 H. Sirringhaus, N. Tessler and R. H. Friend, *Science*, 1998, **280**, 1741.

16 T. Cassagneau and J. H. Fendler, *Adv. Mater.*, 1998, **10**, 877.
17 O. M. Yaghi, H. Li, C. Davis, D. Richardson and T. L. Groy, *Acc. Chem. Res.*, 1998, **31**, 474.
18 M. Antonietti and C. Göltner, *Angew. Chem., Int. Ed. Engl.*, 1997, **36**, 910.
19 M. Templin, A. Franck, D. Chense, H. Leist, Y. Zhang, R. Ulrich, V. Schädler and U. Wiesner, *Science*, 1997, **278**, 1795.
20 A. Van Blaaderen, *Science*, 1998, **282**, 887.
21 S. Oliver, A. Kuperman, N. Coombs, A. Lough and G. A. Ozin, *Nature*, 1995, **378**, 47.
22 S. R. J. Oliver and G. A. Ozin, *J. Mater. Chem.*, 1998, **8**, 1081.
23 S. Oliver, N. Coombs, A. Kuperman and G. A. Ozin, *Adv. Mater.*, 1995, **7**, 931.
24 G. A. Ozin, D. Khushalani, S. Oliver, N. Coombs, G. C. Shen, I. Sokolov and H. Yang, *J. Chem. Soc., Dalton Trans.*, 1997, 3941.
25 G. A. Ozin, *Acc. Chem. Res.*, 1997, **30**, 17.
26 *Art Forms in Nature*, ed. Ernst Haekel, Prestel, Munich, 1998.
27 *On Growth and Form, The Complete Revised Edition*, ed. D'Arcy W. Thompson, Dover, 1992.
28 *Structural Biomaterials*, ed. J. F. V. Vincent, Princeton University Press, Princeton, NJ, 1990.
29 I. Soten and G. A. Ozin, *J. Mater. Chem.*, 1999, **9**, 703.
30 N. Varaksa, N. Coombs, J. E. D. Davies, D. D. Perovic, M. Ziliox and G. A. Ozin, *J. Mater. Chem.*, 1997, **7**, 1601.
31 *Structure and Chemistry of the Apatites and Other Calcium Orthophosphates*, ed. J. C. Elliot, Elsevier, New York, 1994.
32 T. Jiang and G. A. Ozin, *J. Mater. Chem.*, 1997, **7**, 2213.
33 I. Sokolov, T. Jiang and G. A. Ozin, *Adv. Mater.*, 1998, **10**, 942.
34 R. W. J. Scott, M. J. MacLachlan and G. A. Ozin, *Curr. Op. in Solid State Mater. Sci.*, 1999, **4**, 113.
35 M. J. MacLachlan, N. Coombs and G. A. Ozin, *Nature*, 1999, **397**, 681; M. J. MacLachlan, N. Coombs, R. L. Bedard, S. White, L. Thompson and G. A. Ozin, *J. Am. Chem. Soc.*, 1999, **121**, 12005.
36 D. Khushalani, G. A. Ozin and A. Kuperman, *J. Mater. Chem.*, 1999, **9**, 1483.
37 D. Khushalani, Ö. Dag, G. A. Ozin and A. Kuperman, *J. Mater. Chem.*, 1999, **9**, 1491.
38 Ö. Dag, A. Verma, G. A. Ozin and C. T. Kresge, *J. Mater. Chem.*, 1999, **9**, 1475.
39 H. Yang, C. T. Kresge and G. A. Ozin, *Adv. Mater.*, 1998, **10**, 883.
40 G. A. Ozin, *Can. J. Chem.*, 1999, **77**, 2001.
41 S. A. Johnson, D. Khushalani, N. Coombs, T. E. Mallouk and G. A. Ozin, *J. Mater. Chem.*, 1998, **8**, 13.
42 M. J. MacLachlan, P. Aroca, N. Coombs, I. Manners and G. A. Ozin, *Adv. Mater.*, 1998, **10**, 144.
43 Ö. Dag, G. A. Ozin, H. Yang, C. Reber and G. Bussiere, *Adv. Mater.*, 1999, **11**, 474.
44 A. G. Cullis, L. T. Canham and P. D. J. Calcott, *J. Appl. Phys.*, 1997, **82**, 909.
45 G. A. Ozin, E. Chomski, Ö. Dag and A. Kuperman, *Adv. Mater. Chem. Vap. Deposit*, 1996, **2**, 8.
46 G. A. Ozin, Ö. Dag and A. Kuperman, *Adv. Mater.*, 1995, **7**, 72.
47 I. Sokolov, H. Yang, G. A. Ozin and C. T. Kresge, *Adv. Mater.*, 1999, **11**, 636.
48 S. M. Yang, I. Y. Sokolov, N. Coombs, C. T. Kresge and G. A. Ozin, *Adv. Mater.*, 1999, **11**, 1427.
49 S. Inagaki, S. Guan, Y. Fukushima, T. Ohsuna and O. Terasaki, *J. Am. Chem. Soc.*, 1999, **121**, 9611.
50 B. J. Melde, B. T. Holland, C. F. Blanford and A. Stein, *Chem. Mater.*, 1999, **11**, 3302.
51 T. Asefa, M. J. MacLachlan, N. Coombs and G. A. Ozin, *Nature*, 1999, **402**, 867.
52 T. Asefa, M. J. MacLachlan, N. Coombs and G. A. Ozin, *Angew. Chem.*, 1999, in press.
53 C. Ishii, T. Asefa, N. Coombs, M. J. MacLachlan and G. A. Ozin, *Chem. Commun.*, 1999, 2539.
54 O. Dag, C.-Y. Ishii, T. Asefa, M. J. MacLachlan, H. Grondey and G. A. Ozin, *Adv. Mater.*, 1999, submitted.

Paper a905090f